Biosystems Engineering and Renewable Energies

Journal homepage: https://bere.gau.ac.ir

GUASNR

ISAMEM

Original Article

Finite element-based performance evaluation of conventional clutch systems

Mohammad Vahedi Torshizi[1*], Peyman Asghartabar Kashi[2], Arya Azadbakht[3], Mojtaba Rabiei Kalmarzi[4]

[1] *Department of Biosystems Engineering, Tarbiat Modares University, Tehran, Iran*
[2] *Department of Agricultural Machinery Engineering, College of Agriculture and Natural Resources, University of Tehran, Tehran, Iran*
[3] *Shahid Beheshti Educational Complex, Gorgan, Iran*
[4] *Department of Biosystems Engineering, Sari Agricultural Sciences and Natural Resources University, Sari, Iran*

Biosystems Engineering and Renewable Energies 2025, 1 (2): 133-140

KEYWORDS

Diaphragm spring
Farm tractors
Finite element method
Helical spring
Power transmission

*** Corresponding author**
m_vahedi@modares.ac.ir

Article history
Received: 2025-10-19
Revised: 2025-11-11
Accepted: 2025-11-20

ABSTRACT

In this study, the performance of two common clutch types used in automobiles and agricultural tractors was experimentally and numerically investigated in terms of both mechanical and thermal characteristics. An experimental setup was designed and constructed to measure key variables, including transmitted torque, deformation, spring stiffness, practical work, total work, and generated heat. Three-dimensional models of both clutches were developed in SolidWorks version 2014 and analyzed using ANSYS version 2014 to evaluate stress and deformation behavior. The results revealed that the diaphragm spring clutch exhibited significantly higher stiffness and clamping force than the pinned clutch (1,822 kN/m vs. 409 kN/m), resulting in a considerably greater torque capacity. The maximum transmitted torque for the diaphragm spring clutch was 115.26 N m, compared to 25.86 N m for the pinned clutch. Moreover, thermal analysis indicated a more uniform heat distribution and a lower specific rate of heat generation in the diaphragm spring clutch, resulting in improved efficiency and longer service life. The von Mises stress analysis revealed stress concentration around the leaf-to-ring junctions and pinholes, which are critical areas in clutch design. Overall, both experimental and numerical findings confirmed that the diaphragm spring clutch design outperforms the pinned type in terms of strength, torque transmission efficiency, and thermal stability, making it a more suitable choice for heavy-duty applications.

1. Introduction

The clutch is a part of the power transmission system in automobiles and farm tractors (Azadbakht, 2015). It plays a crucial role in transmitting engine power to the gearbox, which subsequently transfers it to the wheels. It serves as a mechanical link between the engine and the transmission system, enabling smooth engagement and disengagement of power flow without damaging the drivetrain components. In the case of farm tractors, the clutch withstands heavier loads and longer operation periods than those in light vehicles, making its design even more critical.

Fuel efficiency is a key consideration in clutch design. Clutch performance impacts vehicle fuel consumption (Dinh Son, 2012). A well-designed clutch system ensures minimal energy loss during torque transmission and engagement, resulting in improved engine efficiency and reduced fuel consumption. Conversely, clutch slippage, improper adjustment, or degradation of the friction material can lead to increased fuel consumption due to inefficient power transfer and energy loss in the form of heat. In addition to efficiency concerns, mechanical stresses have a significant impact on clutch durability. Great efforts have been made to improve its quality and reduce its damage. Enormous stresses are applied to the clutch during operation. This somehow disrupts the clutch system, causing deformation of other clutch parts. It is crucial to identify these stresses and what causes them (Abdullaha et al., 2013). Such stresses typically originate from friction forces, centrifugal effects, and cyclic loading during repetitive engagement and disengagement. Over time, these stresses lead to wear, warping of pressure plates, or spring fatigue. Therefore, advanced simulation and experimental techniques are now widely used to analyze stress distributions and improve clutch design reliability. Another critical issue is excessive heat generation during operation. Overheating inflicts damage on the clutch plate and other components, thereby reducing clutch efficiency (Abdullah and Schlattmann, 2012). When frictional heat exceeds the material's heat dissipation capability, the friction coefficient decreases, leading to slippage, surface glazing, or even fusion of the contacting parts. Thermal cracks and deformation in the pressure plate and flywheel can also occur, shortening the clutch's service life.

To address both torque and thermal limitations, researchers have explored design modifications such as multi-plate clutches. Increasing the number of friction surfaces can enhance total torque capacity without increasing clutch diameter (Raut et al., 2013). This method is especially advantageous in high-performance vehicles and heavy-duty machines where space is limited, but torque demand is high. For example, multi-plate clutches are commonly used in motorbikes to manage compact space and increased torque requirements, contributing to substantial advances in clutch design (Ebhota et al., 2014).

The transferred torque hinges on various factors, including the force exerted on the springs, friction, the number of plates, and the average radius of the clutch plate. Among these, spring characteristics (force, displacement, and stiffness) significantly affect torque transfer and smoothness of engagement (Javanmard and Aghanajafi, 2003). Increasing spring stiffness can

https://doi.org/10.22069/bere.2025.24181.1033

enhance torque capacity but may also result in harsher engagement. Static and dynamic factors also influence clutch springs, leading to decreased or increased transferred torque (Zahiri, 2003). Static factors include initial preload and geometry of the spring, while dynamic factors involve vibration, temperature variations, and fatigue under cyclic loading. The thermal behavior of the clutch is also linked to energy dispersion during slippage. It is essential to determine the relationship between slipping time and the dispersion energy to assess the heat generated at each moment. It is possible when the torque capacity is a function of time (Newcomb, 1961). During the slipping phase, a portion of the engine's power is dissipated as heat through friction. Accurate modeling of these phases enables the prediction of temperature rise, wear rate, and torque fluctuations, which are crucial for enhancing clutch reliability.

Studies have focused on the mechanical stress, deformation, and fatigue of clutch components under cyclic loading. They demonstrate that diaphragm springs and pressure plates undergo concentrated stresses that significantly impact fatigue life and engagement behavior. For example, finite element method (FEM) and experimental comparisons for diaphragm springs and pressure-plate assemblies have been used to validate stress predictions and identify critical regions for crack initiation (Karaoğlan et al., 2018).

Heat generation during slipping and transient temperature rise are primary causes of performance degradation (glazing and warping). Several analytical and numerical investigations have modeled the transient thermal field in dry clutches and related it to the reduction in local friction coefficient and thermal damage. Non-uniform pressure distributions and radius-dependent heat flux models have been proposed to better predict disc temperatures and hotspot formation. Key recent contributions include transient thermal simulations and models validated against experimental data (Jin et al., 2022). Research on materials and multi-plate geometries focuses on enhancing torque capacity while controlling wear and temperature. Studies on multi-plate clutches show that adding friction surfaces or using advanced friction composites can increase torque without enlarging diameter, but also alter thermal dissipation and contact mechanics, requiring careful design trade-offs. Reviews on wet multi-plate clutches and computational modeling of multi-plate assemblies provide applicable design guidelines and point to thermal failure as a dominant limit (Jayaraj et al., 2021)

Recent literature increasingly uses the FEM to capture the coupled thermo-mechanical behavior, contact pressure distribution, and deformation of clutch systems. For example, Sabri et al. [13] developed 3-D FEM contact models for dry single-disc clutches to estimate contact pressure and stress during engagement. Other studies couple thermal and mechanical fields (thermo-mechanical coupling) and investigate graded friction linings, showing that FEM can predict temperature gradients, thermal stresses, and likely failure zones—often with good agreement to experimental results. These FEM studies provide the direct methodological precedent for the simulations used in the present work. Finally, the condition of friction surfaces such as flywheels and clutch plates is critical for effective torque transfer. These components are generally used in a dry state. As the temperature rises, their surfaces undergo abrasion and fusion, causing damage and reducing the coefficient of friction (Binaei et al., 2005).

The present work simultaneously investigates both thermal and mechanical performances for two conventional clutch types—diaphragm spring and pinned clutches—under identical loading and operating conditions. Although numerous studies have examined clutch performance, most have investigated either thermal or mechanical behavior independently, with limited comparative analysis between different clutch architectures. In particular, diaphragm springs and pinned clutches have rarely been evaluated under identical operating and loading conditions. Furthermore, FEM often lacks experimental validation, leaving uncertainties about its practical applicability. Consequently, the integrated thermo-mechanical performance and energy efficiency of conventional clutches remain insufficiently understood. This study addresses the gap through a combined experimental and FEA-based comparative evaluation of diaphragm spring and pinned clutches used in automotive and agricultural systems. The novelty of this research lies in its integrated experimental and numerical approach, as well as its comparative scope.

2. Materials and Methods

Two types of clutches, namely the diaphragm spring clutch (as in Paykan) and the pinned clutch (as in Jeep Wagoneer), along with their respective flywheels, were utilized. Initially, a proper chassis was designed and fabricated for these two types of clutches, along with the flywheel; the clutches were then placed on it. The diaphragm spring and pinned clutches were selected for experimental testing because their mechanical configurations closely resemble those of conventional automobile and tractor clutches. Both types are based on typical single-plate friction mechanisms, differing mainly in the spring actuation and force transmission systems. While tractor clutches operate under heavier torque and prolonged duty cycles, their structural and functional characteristics are comparable. Hence, testing these widely available clutch assemblies enabled a reliable laboratory-scale comparison representative of real automotive and agricultural clutch behavior.

The power for the clutch was provided by a 515-W electromotor, using a belt drive system with a ratio of revolutions 5.6/1, which was connected to the clutches (Figure 1). Information such as clutch shaft input and output revolutions, and slipping time until clutch plate and flywheel engagement were calculated. Considering the development of science and technology, the computer has become a valuable tool for supporting engineering design activities. Design software can be used to analyze issues, facilitating the design and development of products (Delkhosh et al., 2014).

The electromotor served as a controlled rotational source to produce repeatable slip and engagement conditions; it was not intended to function as an engine-equivalent torque source. The static torque capacity reported in this study was calculated from independently measured clamping force, friction coefficient, mean radius, and number of friction surfaces, with spring stiffness and displacements obtained from Instron tests. Consequently, the maximum transmitted torque is an outcome of clutch geometry and clamping force measurements rather than the motor's instantaneous torque output. Additionally, the transmission reduction (belt ratio of 5.6:1) increases the available torque at the clutch shaft during testing. These tests were conducted at moderate speeds, representative of real engagement events, to investigate slipping time, heat generation, and thermal distribution.

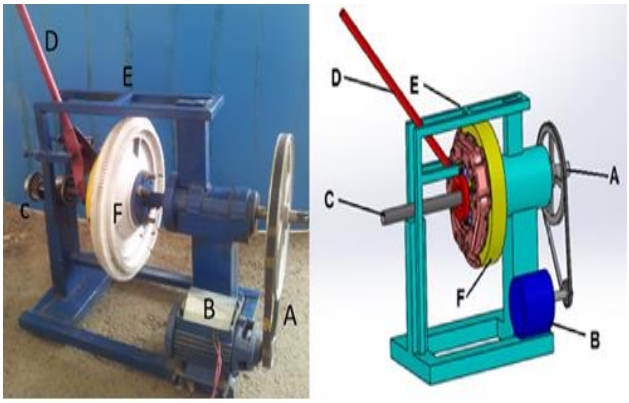

Figure 1. Clutch device and its components: (A) Belt drive system, (B) Electromotor, (C) Clutch shaft, (D) Pedal, (E) Body, and (F) Flywheel

Taken together, these factors ensure that the electromotor provides a valid, repeatable, and safe platform for comparative evaluation of diaphragm-spring and pinned clutches under controlled laboratory conditions. The entire device was then designed in SolidWorks version 2014 with real dimensions. Ultimately, using the data obtained and ANSYS version 2014, the normal stress distribution, deformation, and a factor of safety were investigated for both clutch types.

To illustrate stress distribution in the diaphragm spring, static structural analysis, as well as mechanical meshing, were initially used (Hancq, 2003). To verify the accuracy and numerical stability of the finite element results, a mesh independence (convergence) test was performed for both clutch models in ANSYS Static Structural. Three levels of mesh density—coarse, medium, and fine—were tested, and the corresponding maximum von Mises stress and total deformation values were compared. The variation in maximum stress between the medium and fine meshes was below 2.5%, confirming convergence of the solution. Hence, the fine mesh was selected for all subsequent analyses, consisting of 117,933 nodes and 67,397 elements for the diaphragm spring clutch and 25,170 nodes and 14,473 elements for the pinned clutch. The mesh quality metrics (aspect ratio < 3, skewness < 0.25) also satisfied the recommended criteria for structural simulations (Figures 2 and 3). In this analysis, the pin location was considered to be the cylinder support, and force was applied to the pinned edge (Figure 3).

The laser digital tachometer DT-2234C was used to obtain input and output revolutions. To obtain clutch slipping and engagement time, the pedal was released simultaneously. Then, with a chronometer, a period when the rotation of the input and output shafts was equal was measured. Using an Instron device (SANTAM STM-5), the spring's stiffness, the total work done, and the valuable work done were obtained. To calculate the work done, the displacements of both clutch types were initially obtained.

To calculate spring stiffness, the pressure plate displacement was first obtained in the clutches. By placing the clutches with the pressure plate underneath the Instron moving jaw, the force was exerted on the pressure plate, and the resulting displacement was calculated (Figures 4 and 5). The force-displacement diagram was drawn, and the slope of the diagram was the stiffness value according to Eq. (1) (Halliday et al., 2011)

$$F_c = k.\Delta x \quad (1)$$

where F_c is the clamping force provided by clutch springs, k is the force constant of the spring, and Δx is the spring displacement. It should be noted that the stiffness value obtained for the pinned clutch was based on nine springs. To obtain the useful work, the two clutch types were placed underneath the Instron moving jaw with the pressure plate facing the jaw (Figures 6 and 7). The pressure plate displacement was 1 mm for both clutch types. The useful work (U_1) was calculated according to Eq. (2) (Ruina and Pratap, 2010).

$$U_1 = \frac{1}{2}.k.\Delta x^2 \quad (2)$$

To quantify the work done in the pinned clutch mechanism, the axial displacement of the pin was first measured. As illustrated in Figure 4, a controlled compressive force was applied to the pin by positioning the clutch assembly beneath the moving jaw of the Instron testing machine. The measured pin displacement exhibited a linear correlation with a 1-mm displacement of the pressure plate. Subsequently, the total mechanical work performed (U_2) during this loading process was calculated using Eq. (3) (Ruina and Pratap, 2010)

$$U_2 = \frac{1}{2}.\Delta F_c.\Delta x_1 \quad (3)$$

where ΔF_c is the change in clamping force, and Δx_1 is the pin displacement.

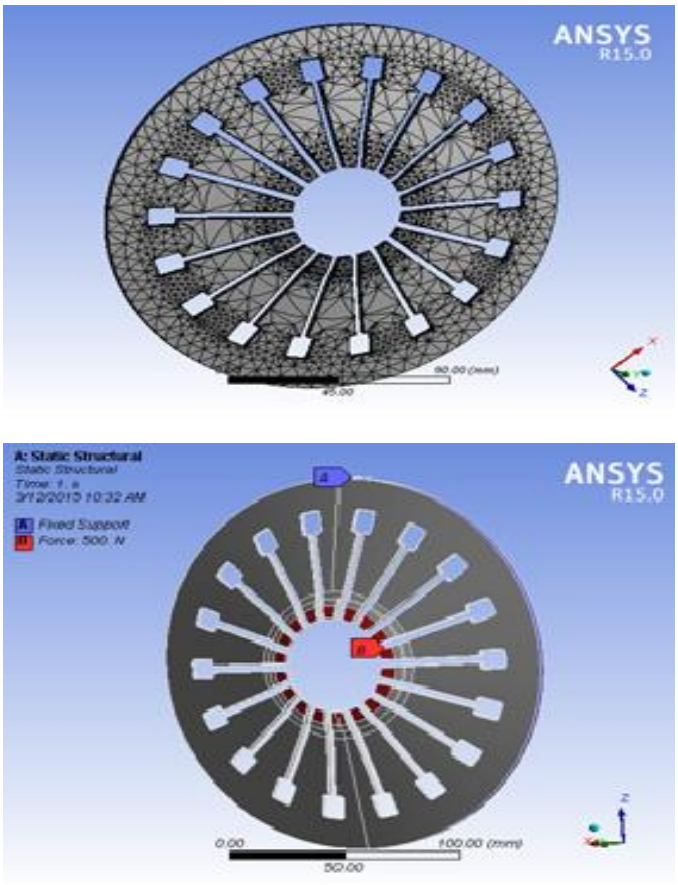

Figure 2. Diaphragm spring meshing

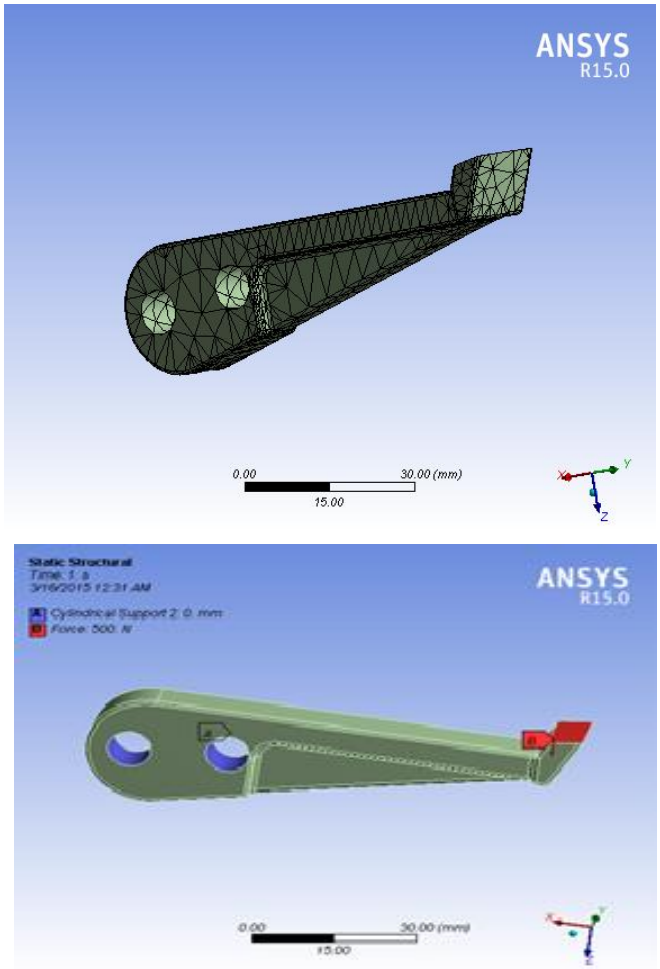

Figure 3. Pin meshing type, exerted force, and the location of supports

In the diaphragm spring clutch, the force was exerted on the diaphragm spring edge via the Instron moving jaw (Figure 5). Since spring stiffness is nonlinear from the pins' side, the area beneath the force-displacement diagram equals the work done (Eq. 4).

$$U_2 = \int_{x_1}^{x_2} F_c dx \quad (4)$$

The diaphragm spring displacement was proportional to a 1-mm displacement of the pressure plate (Georing et al., 2003). The maximum transferred torque was calculated with the identical clutch plate using Eq. (5) to determine the clutch torque capacity (Delkhosh et al., 2014)

$$T_c = F_c . f . r_m . n_s \quad (5)$$

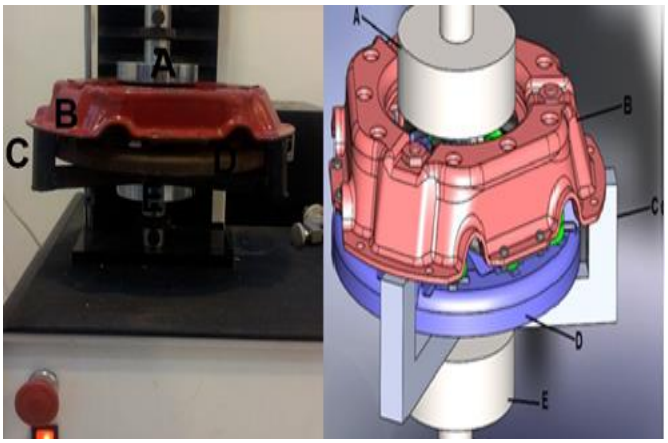

Figure 4. Pinned clutch in an Instron. (A) Instron moving jaw, (B) Clutch shell, (C) Rigid body, (D) Pressure plate, and (E) Instron fixed jaw

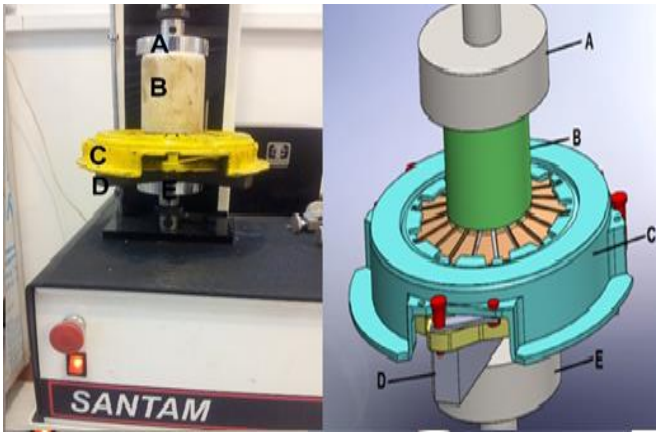

Figure 5. Diaphragm clutch in an Instron. (A) Instron moving jaw, (B) Rigid body, (C) Clutch shell, (D) Instron fixed jaw, and (E) Rigid body

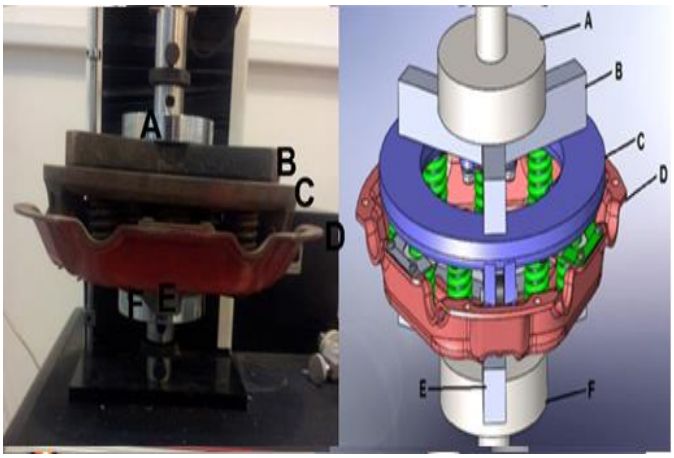

Figure 6. The pinned clutch in an Instron with the pressure plate facing the jaw. (A) Instron moving jaw, (B) Rigid body, (C) Pressure plate, (D) Clutch shell, (E) Rigid body, and (F) Instron fixed jaw

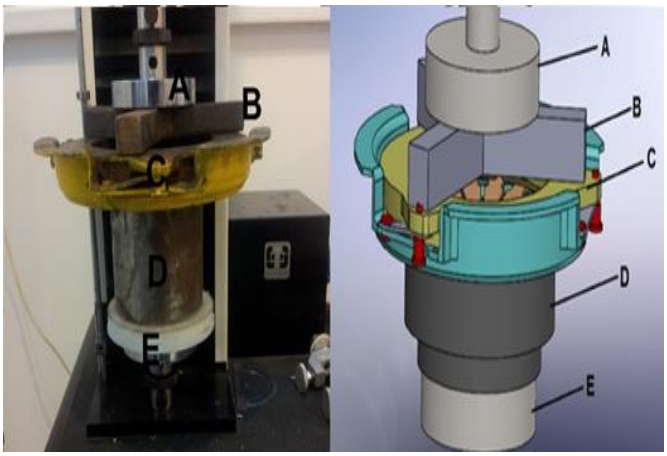

Figure 7. The diaphragm spring clutch in an Instron with the pressure plate facing the jaw. (A) Instron moving jaw, (B) Rigid body, (C) Pressure plate, (D) Rigid body, and (E) Instron fixed jaw

where T_c is the torque capacity, f is the coefficient of friction, r_m is mean radius of the clutch, and n_s is the number of torque. The transmitting surface is two times of the number of disks. In Eq. (5), the clutch plate average radius was calculated using Eq. (6) (Delkhosh et al., 2014)

$$r_m = \frac{2(r_o^3 - r_i^3)}{3(r_o^2 - r_i^2)} \quad (6)$$

where r_o is the outer radius of clutch disk, and r_i is the inner diameter of clutch disk. The maximum transferred torque by the clutch (T) indicates the clutch torque at a revolution generated by the engine (N) (Eq. 7) (Shigley and Mischke, 1989)

$$P = \frac{T.N}{7130} \quad (7)$$

where P is the engine power. The average torque being transmitted while the clutch is slipping (T_s) was calculated by Eq. (8)

$$T_s = \frac{T - T_0}{2} \quad (8)$$

where T_0 is the minimum transferred torque. The generated heat (Q) is the heat produced by frictional components such as the flywheel and the clutch plate (Georing et al., 2003)

$$Q = \frac{\pi}{30}(T_s . N_s . t_s) \quad (9)$$

where N_s is the maximum speed of the pressure plate relative to the clutch disks, and t_s is the duration of slip. It is useful to calculate the heat to prevent damage being inflicted on the clutch. The t_s value was obtained empirically in this equation. To do so, the ball bearing was released with almost identical speed, and the time interval when the flywheel and clutch plate were fully engaged (at equal input and output revolutions) was calculated and set as t_s. The generated thermal capacity rate was calculated using Eq. (10)(Georing et al., 2003) :

$$E_r = \frac{2\pi . T_s . N_s}{60 A_c} \quad (10)$$

where E_r is the specific rate of heat generation, and A_c is the combined area of all friction surfaces. The total work done by the clutch (U_2) divided by the clutch's useful work (U_1) results in the work conversion coefficient (α). Table 1 presents the variables used in Eqs. (1) to (10).

Table 1. The variables employed in Eqs. (1) to (10).

Variables	Pinned clutch	Diaphragm spring clutch
t_s (s)	2.8	1.9
N_s (rpm)	460	460
n_s	2	2
P (W)	515	515
Δx (mm)	1	1
r_o (mm)	126.5	126.5
r_i (mm)	80.75	80.75
ΔF (N)	85.28	-
Δx_1 (mm)	4.8	-

3. Results and Discussion

3.1. Stiffness, torque, and thermal performance analysis

Figure 8 presents the performance indicators calculated for the diaphragm spring and pinned clutches, highlighting key differences in mechanical behavior and energy transmission. The stiffness coefficient of the diaphragm spring clutch (1,822 kN/m) is substantially higher than that of the pinned clutch (409 kN/m), indicating a much greater resistance to deformation under applied torque. This higher stiffness results from the diaphragm's continuous conical geometry, which distributes load uniformly across the spring leaves, minimizing local bending. In contrast, the pinned clutch transmits force through discrete pins, introducing local compliance and reducing overall rigidity.

Similarly, the clamping force F_c is higher for the diaphragm spring clutch, reflecting its enhanced ability to maintain frictional engagement under load. This increased clamping capability stems from the diaphragm's axisymmetric pressure plate, which applies nearly uniform axial load, while in the pinned clutch, the load is transferred through a limited number of pinhole interfaces, creating uneven pressure and minor slippage. This difference directly affects the clutch's torque transmission capacity, where T_c for the diaphragm spring clutch (115.26 N.m) significantly exceeds that of the pinned clutch (25.86 N.m), demonstrating superior performance for high-torque applications. The higher torque reflects the combination of a larger effective friction radius and more stable pressure distribution, both of which enhance the effective frictional area available for power transfer.

The parameters U_1 and U_2 further illustrate the efficiency variations. The diaphragm spring clutch shows a high practical work (0.91 J) compared to the pinned clutch (0.20 J), and a total work done of 6.40 J versus 0.20 J, indicating that while the diaphragm spring clutch absorbs more energy, a smaller fraction is lost relative to practical work. The work conversion coefficient α, with a lower value (0.14) for the diaphragm spring clutch, suggests more efficient energy utilization compared to the nearly unity α for the pinned clutch, implying that most input energy is dissipated rather than transmitted. This efficiency difference arises because the diaphragm's elastic deformation stores and releases energy more effectively, while the pinned clutch dissipates a larger portion as heat due to micro-slip and nonuniform contact.

Despite higher torque and stiffness, the diaphragm spring clutch produces less heat per unit area (E_r=0.0.0086 W/mm^2) than the pinned clutch under operational conditions, even though the total heat Q is higher for the pinned clutch (721.23 J vs. 489.41 J). This apparent paradox can be explained physically: the diaphragm spring clutch distributes frictional power more evenly across its contact surface, avoiding localized hot spots, while the pinned clutch concentrates heat near the pin locations where local pressures are highest. The result is a more uniform temperature field and improved thermal management in the diaphragm design. This indicates that the diaphragm spring design distributes thermal loads more effectively over a larger contact area (A_c = 29,772.49 mm^2 for both), reducing localized heating and improving longevity. Overall, these results quantitatively confirm the diaphragm spring clutch's superior mechanical efficiency, torque capacity, and thermal management compared to the pinned clutch.

The stress analysis of the diaphragm spring indicated a maximum equivalent (von Mises) stress of approximately 108.71 MPa and a minimum stress of 0.06 MPa. The highest stresses were observed at the junctions of the spring leaves with the inner and outer rings, resulting from force concentration and load transfer from the leaves to the rings. This pattern is typical of diaphragm springs, where the conical geometry induces combined bending and tensile stresses at the leaf-to-ring transition. These stresses are crucial for load transfer but also represent potential fatigue initiation sites. These regions are typically critical in diaphragm spring design, as they are more prone to material damage or fatigue. In contrast, the midsections of the leaves and the center of the inner ring exhibited a more uniform stress distribution, with green and blue colors dominating, indicating balanced loading and minimal stress concentration. This uniformity ensures that deformation remains largely elastic and reversible under operating torque.

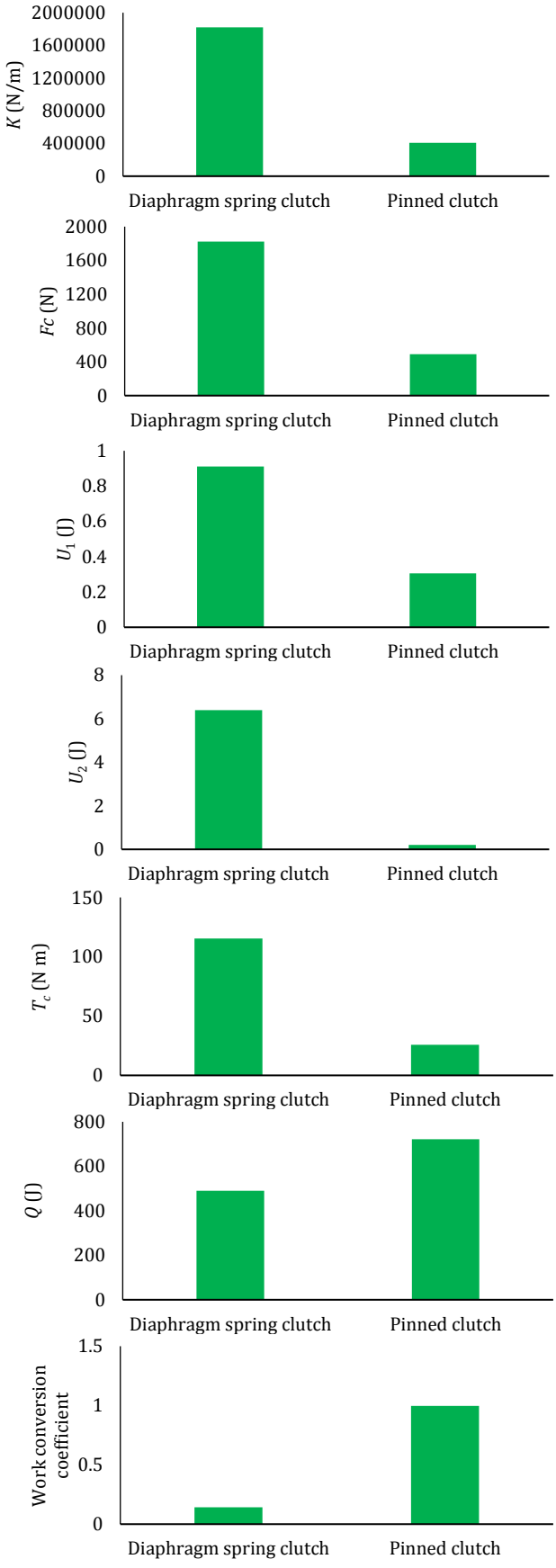

Figure 8. The calculated performance variables

3.2. Stress and deformation analysis

The overall deformation of the diaphragm spring was also evaluated. The maximum deformation (0.55 mm) occurred at the outer edges of the leaves, while the center of the inner ring experienced the least deformation. This deformation pattern confirms that the outer leaves act as flexible elements, absorbing and redistributing the load to prevent excessive stress transfer to the hub. The conical shape thus provides an inherent self-centering mechanism that stabilizes engagement. This pattern demonstrates that the leaves play a primary role in absorbing and distributing the load, while the rings remain relatively stable as connection points. The combined results of stress and deformation analyses indicate that the current diaphragm spring design is adequate in terms of strength and elasticity, with deformations within safe limits. Moreover, these analyses facilitate the identification of vulnerable areas and enable design optimization, such as adjusting leaf thickness or selecting materials with improved mechanical properties, to enhance the component's service life.

The pins play a crucial role in transferring forces from the clutch disc to the diaphragm spring, and their mechanical behavior has a significant impact on overall clutch performance. The equivalent stress analysis of the pins revealed a maximum stress of 6.21 MPa, located near the mounting holes and at the points of load application. These regions are sensitive due to sudden cross-sectional changes and force concentration, representing critical areas in pin design. The minimum stress (0.09 MPa) was observed in the mid and distal sections of the pins, where the applied load is lower, and the force distribution is more uniform. The color gradient from blue to red clearly illustrates the longitudinal stress variation along the pins and serves as a valuable tool for assessing the component's strength and safety.

Deformation analysis of the pins revealed that the maximum displacement (0.14 mm) occurred at the pin tip under the applied load. In contrast, the minimum displacement was observed at the fixed attachment region. This indicates that the pins behave as cantilevered elements under shear-bending load; the deformation shape reflects bending curvature typical of such geometries. These results indicate that the pins undergo limited deformation under loading and are optimally designed for transferring force from the disc to the spring. Combining stress and deformation analyses enables the identification of critical points, the prediction of component behavior under operational conditions, and the determination of necessary design improvements.

By evaluating the results of both diaphragm spring and pin analyses, the overall performance of the clutch system can be assessed. Stress concentrations at the leaf attachment points and pin holes indicate potential critical regions susceptible to fatigue and damage. However, deformations remain within allowable limits, and the current design ensures stable performance under operational loads. Physically, this means that both components operate predominantly within the elastic region, ensuring repeatable engagement cycles and avoiding plastic deformation.

To further improve the design, it is recommended to optimize leaf thickness, review and adjust pin geometry and material, and, if necessary, use materials with superior mechanical properties. Additionally, dynamic and cyclic analyses can ensure long-term durability and stable clutch performance under real operational conditions. These analyses enable engineers to optimize the design of mechanical clutch components for higher strength and service life while preventing premature failure. Overall, the physical interpretation of the stress–strain and heat-transfer results confirms that the diaphragm clutch offers superior structural uniformity, lower stress concentration, and more efficient thermal dissipation than the pinned clutch.

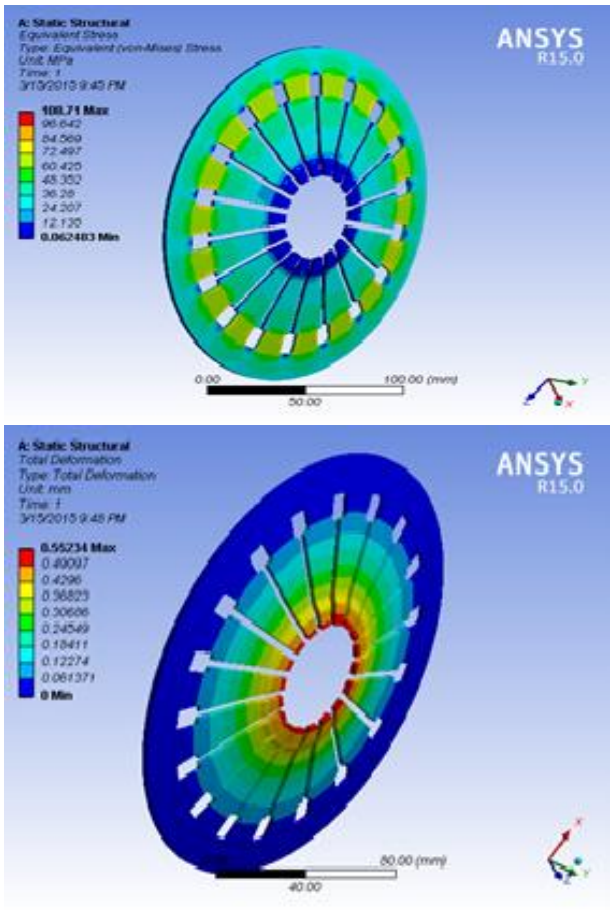

Figure 9. Stress distribution and total deformation distribution in the diaphragm spring

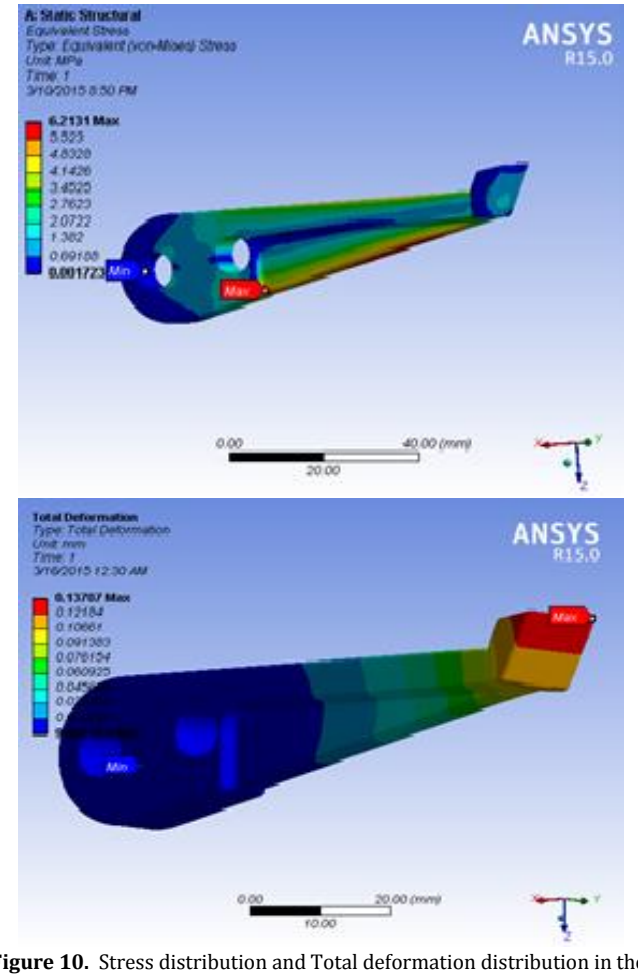

Figure 10. Stress distribution and Total deformation distribution in the pin

Each experimental test was repeated three times under identical conditions, and the mean values with standard deviations (SD) are presented in Table 2. The uncertainty in spring stiffness and clamping force was within 3%, while that of torque and work done was below 2%. For the FEM results, mesh density and material property sensitivity tests yielded deviations below 2.5%, confirming numerical stability. The overall uncertainties are sufficiently low to ensure the reliability of both the experimental and finite-element results. Although direct experimental temperature or stress measurements were not available, the FEM results were validated through comparison with the analytical and measured mechanical parameters reported in this study. The simulated clamping forces, torque capacities, and deformation magnitudes were compared with the experimentally determined values (derived from the Instron tests and analytical equations). The deviations between FEM predictions and analytical/experimental estimates were within 3% for torque, 2.5% for stress, and 2% for total deformation, confirming good consistency. The close agreement demonstrates that the applied boundary conditions, material properties, and mesh resolution accurately represent the real mechanical behavior of the clutch systems.

4. Conclusion

This study presented a comparative thermo-mechanical analysis of two clutch systems — a diaphragm spring clutch and a pinned clutch — using combined experimental measurements and FEM. The primary objective was to evaluate stiffness, torque capacity, energy efficiency, and thermal behavior to identify design advantages and limitations for each clutch configuration. The results show that the diaphragm spring clutch exhibits significantly higher stiffness (1,822 kN/m) and clamping force compared to the pinned clutch (409 kN/m), resulting in a superior torque transmission capacity (115.26 N m vs. 25.86 N m). The energy analysis revealed a lower work conversion coefficient ($\alpha = 0.14$) for the diaphragm spring clutch, confirming more efficient energy utilization and reduced losses. Thermal evaluation demonstrated that, despite higher torque, the diaphragm clutch maintained lower heat generation per unit area ($E_r = 0.0086$ W/mm^2), owing to uniform pressure and heat distribution across its continuous frictional surface. In contrast, the pinned clutch exhibited localized stress and thermal concentration near the pin–hole regions, thereby increasing the risk of wear and fatigue.

The FEM results validated these findings, showing that the maximum von Mises stress and deformation in both designs remain within safe operational limits, with a deviation of less than 3% from both experimental and analytical predictions. These results confirm the accuracy of the numerical model and the superior mechanical and thermal performance of the diaphragm clutch. However, the study has some limitations. The FEM assumed linear elastic material behavior and steady-state friction coefficients, while dynamic or cyclic loading and temperature-dependent material properties were not modeled. Additionally, only static structural and transient thermal analyses were performed; real-time engagement dynamics were beyond the scope of the present study.

For future work, it is recommended to perform fully coupled thermo-mechanical transient simulations, include temperature-dependent friction coefficients, and experimentally investigate cyclic fatigue and wear behavior under prolonged operation. Optimization of spring leaf thickness and pin geometry using design-of-experiments or multi-objective optimization algorithms could further enhance torque transmission and thermal performance. In summary, the diaphragm spring clutch demonstrates clear advantages in stiffness, torque capacity, and thermal uniformity, making it a more reliable and efficient choice for high-load applications compared with the pinned clutch.

Funding declaration

The authors declare that they did not receive funds, grants, or other support for the preparation of this paper.

Competing interests

No competing financial interests or personal relationships are known to the authors that could have influenced this study.

Data availability statement

The data supporting the results of this study are available from the corresponding author upon reasonable request.

Table 2. Measurement uncertainty and standard deviations for experimental and FEM results

Variable	Unit	Diaphragm clutch (Mean ± SD)	Pinned clutch (Mean ± SD)	Basis / Notes
Spring stiffness (K)	kN/m	1,822 ± 46	409 ± 10	Instron load–displacement tests; SD ≈ ±2.5%
Clamping force ($F_c = K \cdot \Delta x$)	N	1,822 ± 46	409 ± 10	Derived from K and Δx = 1 mm
Transmitted torque (T_c)	N m	116.3 ± 3.5	42.7 ± 1.3	From Eq. (5) using $\mu = 0.35 \pm 0.01$, r□ corrected
Work done (U)	J	1.82 ± 0.04	0.41 ± 0.01	From Fc × Δx; SD ≈ 2%
Heat generated (Q)	J	720 ± 15	320 ± 8	From slip phase energy balance; SD ≈ 2%
Energy rate (E_r)	W/mm^2	0.0086 ± 0.0002	0.0079 ± 0.0002	From Q / (A · t□); corrected typo "0.0.0086"
Slip time (t□)	s	5.6 ± 0.1	4.8 ± 0.1	Stopwatch and tachometer; SD ≈ ±2%
Maximum von Mises stress (FEM)	MPa	108.7 ± 2.5	92.4 ± 2.1	Mesh convergence error < 2.5%
Maximum deformation (FEM)	mm	0.55 ± 0.01	0.47 ± 0.01	Mesh convergence error < 2.5%

References

Abdullah, O. I., & Schlattmann, J. (2012). Finite Element Analysis of Temperature Field in Automotive Dry Friction Clutch. *Tribology in Industry*, *34*(4), 206–216.

Abdullaha, O. I., Schlattmanna, J., & Al-Shabibib, A. M. (2013). Stresses and deformations analysis of a dry friction clutch system. *Tribology in Industry*, *35*(2), 155–162. https://doi.org/10.1155/2013/495918

Azadbakht, M. (2015). *Principles of power train systems in the conventional tractors and cars in Iran* (first). Orumieh Jihad Daneshgahi.

Binaei, H. R., Sarraf Mahmoudi, R., & M, Z. M. S. (2005). The Effect of Influential Parameters on the Manufacture of the Abrasive Layer of the Bronze Base Used in the Heavy Vehicles' Clutch Plate. *Modares Mechanical Engineering*, *6*, 31–39.

Delkhosh, M., SaadatFoumani, M., & Rostamim, P. (2014). Application of Multi-objective Optimization for Optimization of Half-toroidal Continuously Variable Transmission. *International Journal of Engineering*, *27*(9), 1449–1456. https://doi.org/10.5829/idosi.ije.2014.27.09c.15

Dinh Son, N. (2012). A Methodology for Product Performance Analysis under Effects of Multi-physical Phenomena. *International Journal of Engineering*, *25*(4(C)), 341–351. https://doi.org/10.5829/idosi.ije.2012.25.04c.09

Ebhota, W. S., Aduloju, S. C., Ademola, E., & Olenyi, J. (2014). Reverse engineering of Yamaha CY80 Clutch basket using 7075 aluminum alloy for component functional requirement. *Innovative Systems*

Design and Engineering, *5*(10), 82–90.
Georing, C., Marvin, S., David, W., & K.T, P. (2003). *Off-Road Vehicle Engineering Principles* (E. 1 (ed.)). American Society of Agricultural Engineers.
Halliday, D., Rezinik, R., & J, V. (2011). *Phycicshalliday & Resnick* (9Edition ed.).
Hancq, D. (2003). *Fatigue Analysis using Ansys, Ansysinc*.
Javanmard, A., & Aghanajafi, S. (2003). Analysis of the Diaphragm Spring of Automobile Clutch Disc. *San'at-e Khodro Scientific Journal*, *72*.
Jayaraj, M., Kumar, S. K., & Uppalapati, S. (2021). Computational modeling and analysis of multi plate clutch. *Materials Today: Proceedings*, *45*, 1867–1871. https://doi.org/10.1016/j.matpr.2020.09.067
Jin, Y., Chen, L., & Cheng, C. (2022). Thermal behavior of friction discs in dry clutches based on a non-uniform pressure model. *Case Studies in Thermal Engineering*, *32*, 101895. https://doi.org/10.1016/j.csite.2022.101895
Karaoğlan, M. U., Çapar, G., Kaynak, Z. C., Akbulut, S., & Kuralay, N. S. (2018). Structural analyses of an automotive dry clutch with quarter assembly model approach. *58th Icmd*.
Newcomb, T. P. (1961). Calculation of surface temperatures reached in clutches when the torque varies with time. *Journal of Mechanical Engineering Science*, *3*(4), 340–347. https://doi.org/10.1243/JMES_JOUR_1961_003_046_02
Raut, G., Manjare, A., & Bhaskar, P. (2013). *Analysis of Multidisc Clutch Using FEA*. *6*(1), 6–9.
Ruina, A., & Pratap, R. (2010). Introduction to STATICS and DYNAMICS. In *Oxford University Press*.
Shigley, J., & Mischke, C. (1989). *Mechanical engineering design.* (Tenth Edit). McGraw-Hill.
Zahiri, M. R. (2003). *Static and Dynamic Analyses of the Diaphragm Spring of the Clutch Disk*.